Nef homodimers down-regulate SERINC5 by AP-2–mediated endocytosis to promote HIV-1 infectivity

Received for publication, June 2, 2020, and in revised form, August 24, 2020 Published, Papers in Press, September 1, 2020, DOI 10.1074/jbc.RA120.014668

Ryan P. Staudt and Thomas E. Smithgall*

From the Department of Microbiology and Molecular Genetics, University of Pittsburgh, School of Medicine, Pittsburgh, Pennsylvania, USA

Edited by Craig E. Cameron

SERINC5 is a multipass intrinsic membrane protein that suppresses HIV-1 infectivity when incorporated into budding virions. The HIV-1 Nef virulence factor prevents viral incorporation of SERINC5 by triggering its down-regulation from the producer cell membrane through an AP-2–dependent endolysosomal pathway. However, the mechanistic basis for SERINC5 down-regulation by Nef remains elusive. Here we demonstrate that Nef homodimers are important for SERINC5 down-regulation, trafficking to late endosomes, and exclusion from newly synthesized viral particles. Based on previous X-ray crystal structures, we mutated three conserved residues in the Nef dimer interface (Leu^{112}, Tyr^{115}, and Phe^{121}) and demonstrated attenuated homodimer formation in a cell-based fluorescence complementation assay. Point mutations at each position reduced the infectivity of HIV-1 produced from transfected 293T cells, the Jurkat TAg T-cell line, and donor mononuclear cells in a SERINC5-dependent manner. In SERINC5-transfected 293T cells, virion incorporation of SERINC5 was increased by dimerization-defective Nef mutants, whereas down-regulation of SERINC5 from the membrane of transfected Jurkat cells by these mutants was significantly reduced. Nef dimer interface mutants also failed to trigger internalization of SERINC5 and localization to Rab7^{+} late endosomes in T cells. Importantly, fluorescence complementation assays demonstrated that dimerization-defective Nef mutants retained interaction with both SERINC5 and AP-2. These results show that down-regulation of SERINC5 and subsequent enhancement of viral infectivity require Nef homodimers and support a mechanism by which the Nef dimer bridges SERINC5 to AP-2 for endocytosis. Pharmacological disruption of Nef homodimers may control HIV-1 infectivity and viral spread by enhancing virion incorporation of SERINC5.

The HIV-1 Nef accessory protein is expressed early in the HIV-1 life cycle where it promotes viral replication and AIDS progression (1). Sole expression of Nef within the CD4-positive cell compartment induces an AIDS-like syndrome in transgenic mice (2). Conversely, patients harboring Nef-defective strains of HIV-1 exhibit reduced viral loads and delayed progression to AIDS (3, 4). Enhancement of lentiviral pathogenicity by Nef is conserved across species. Disruption of the *nef* ORF of simian immunodeficiency virus (SIV) significantly reduces viral replication and prevents the development of AIDS-like disease in SIV-infected macaques (5). These are just a few examples of the evidence supporting a central role for Nef in HIV-1 and SIV pathogenicity.

Nef is a small protein (molecular mass range of 27–34 kDa, depending on the viral subtype) that is associated with host cell membranes by virtue of N-terminal myristylation (6). Nef lacks inherent enzymatic activity, functioning instead through multiple protein–protein interactions that alter host cell signaling and protein trafficking networks involving as many as 70 host cell proteins (7). Nef selectively binds and activates members of the Src and Tec protein-tyrosine kinase families (8–11). Disruption of Nef-dependent kinase activation through genetic or pharmacological means impairs Nef-mediated enhancement of HIV-1 infectivity and replication (10–14). In terms of protein trafficking, Nef drives the down-regulation of cell-surface receptors essential for immune recognition and viral entry, including MHC-I, CXCR4, CCR5, and CD4 (6, 15, 16). Receptor down-regulation involves Nef interactions with endosomal trafficking proteins including the adaptor protein complexes 1 and 2 (AP-1 and AP-2) (17, 18). Down-regulation of CD4 requires simultaneous engagement of Nef with both the cytoplasmic tail of CD4 and a hemicomplex formed by the α and σ2 subunits of AP-2 (19). Nef–CD4–AP-2 complexes form clathrin-coated pits at the cell surface, leading to endocytosis and lysosomal degradation of internalized CD4 (20).

Nef-mediated endocytosis of the SERINC5 restriction factor, a process essential for enhancement of HIV-1 infectivity, is also mediated by the AP-2 trafficking pathway. In the absence of Nef, SERINC5 is present on the surface of HIV-1–infected cells and incorporated into the membrane of newly synthesized virions (21–23). Incorporation of SERINC5 disrupts viral fusion with host cells and delivery of the viral core through a cryptic, Env-dependent mechanism. Nef antagonizes SERINC5 in part by promoting AP-2–dependent down-regulation of SERINC5 from the plasma membrane of infected cells, thereby preventing incorporation into budding virions (22). Following down-regulation by Nef, internalized SERINC5 is targeted for degradation via the endolysosomal pathway (24).

Although Nef uses distinct structural motifs to recognize diverse host cell partners, many Nef functions also require homodimer formation. Mutants of Nef that are defective for homodimerization are unable to induce host-cell tyrosine-kinase activation, even though they retain interaction with the kinase proteins (11). This observation is consistent with the formation of Nef–kinase dimer complexes necessary for kinase activation by transautophosphorylation. Dimerization-defective

* For correspondence: Thomas E. Smithgall, tsmithga@pitt.edu.

Nef mutants are also unable to down-regulate CD4 from the host-cell surface, and these mutations reduce HIV-1 replication efficiency in cell lines (25, 26).

In this study, we investigated the role of Nef homodimerization in HIV-1 infectivity and restriction by SERINC5. Using a series of Nef mutants defective for homodimer formation in cells, we demonstrated that Nef dimers enhance infectivity of HIV-1 produced from T-cell lines and donor PBMCs, as well as 293T cells co-transfected with SERINC5. These same Nef mutants were attenuated in their ability to exclude SERINC5 from newly synthesized virions. Impairment of Nef dimerization reduced down-regulation of SERINC5 from the cell surface and prevented intracellular trafficking to Rab7+ late endosomes. Critically, cell-based fluorescence complementation assays revealed that these Nef mutants retained interaction with both SERINC5 and the AP-2 α and σ2 subunits, indicating that the reduced antagonism of SERINC5 was not due to the loss of Nef association with either partner protein. Taken together, our data demonstrate that Nef antagonizes the SERINC5 restriction factor as a homodimer, which may serve as a bridge linking SERINC5 with AP-2 for endocytosis and degradation.

Results

Structural basis of HIV-1 Nef homodimerization

In this study, we explored the role of Nef homodimerization in the down-regulation of SERINC5 and promotion of HIV-1 infectivity using a genetic approach involving Nef mutants defective for homodimer formation. X-ray crystallography of Nef in complex with the regulatory SH3 and SH2 domains of Src-family kinases has shown that Nef forms homodimers through a hydrophobic interface involving side chains of residues in the Nef αB helices and adjacent loops (27, 28). An example is provided by the structure of HIV-1 Nef in complex with the SH3–SH2 regulatory region of the Src-family kinase, Hck (PDB code 4U5W; a model of the Nef homodimer is shown in Fig. 1*A*) (28). In this structure, three conserved residues from one Nef subunit (Leu^{112}, Tyr^{115}, and Phe^{121}) converge to create a "hydrophobic cup" that clasps the side chain of Val^{70} from the opposing Nef monomer in a reciprocal fashion (Fig. 1*B*). A recent study has shown that recombinant Nef proteins in which Leu^{112} or Tyr^{115} is replaced with aspartate or in which Phe^{121} is substituted with alanine fail to form dimers in solution, providing direct evidence that these residues are essential for dimer stabilization (11). Mutations at these positions attenuate multiple Nef functions, including host-cell kinase activation, enhancement of HIV-1 replication, and receptor down-regulation including CD4 (see the introduction).

Although the role of Nef homodimers in SERINC5 antagonism has not been explored, the mechanistic similarity between Nef-mediated down-regulation of CD4 and SERINC5 suggests a key role. Both processes involve clathrin-mediated endocytosis via the tetrameric trafficking adaptor protein AP-2, which interacts directly with Nef through a hemicomplex of its α and σ2 subunits (19, 29). Alignment of the Nef 4U5W homodimer with the crystal structure of Nef bound to the AP-2 α/σ2 hemicomplex shows that the Nef homodimer interface residues do not contact AP-2 (Fig. 1*C*), suggesting that the dimer interface mutations described above will not affect AP-2 recruitment.

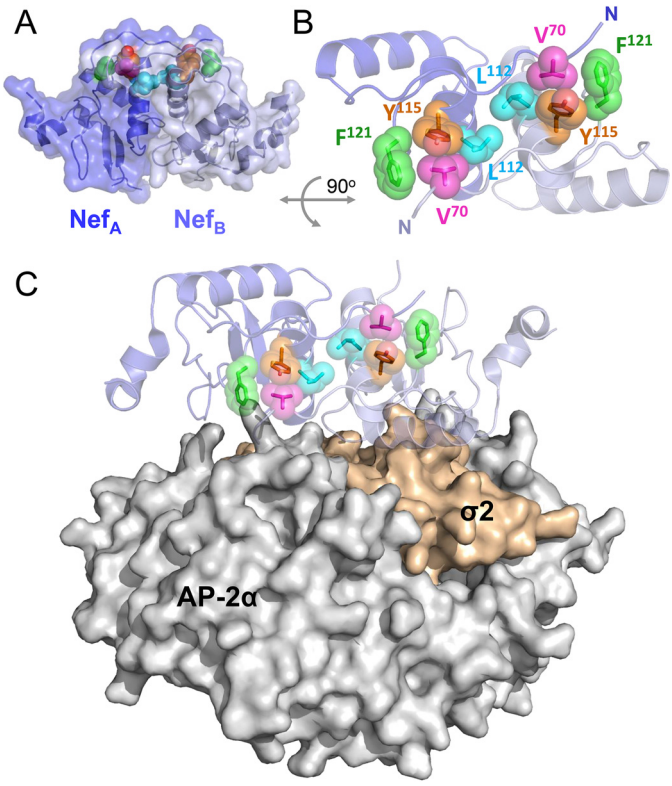

Figure 1. Structural basis of Nef dimerization. *A*, overall structure of the HIV-1 Nef homodimer present in the 2:2 heterocosmplex with the Hck SH3–SH2 regulatory domain proteins (PDB code 4U5W; the SH3–SH2 proteins are not shown for clarity). The Nef monomers (Nef$_A$ and Nef$_B$) are rendered in *dark* and *light blue*, respectively. *B*, zoomed and rotated view of the Nef dimerization interface in which conserved residues Leu^{112}, Tyr^{115}, and Phe^{121} (*cyan*, *orange*, and *green*, respectively) form a hydrophobic cup around Val^{70} (*pink*) from the opposing monomer. *C*, one Nef monomer from the homodimer shown in *A* was aligned with Nef in complex with the AP-2 α/σ2 hemicomplex (PDB code 4NEE). The AP-2 α and σ2 subunits are shown as surfaces in *gray* and *light orange*, respectively. This alignment shows that the Nef homodimer interface is structurally distinct from the point of contact with AP-2, which involves the Nef internal loop (not shown).

These mutants were therefore chosen to explore the requirement for Nef dimers in SERINC5 regulation.

Although Nef is present in HIV-1 virions and expressed early within the viral life cycle (29), previous analyses have examined the impact of mutations on Nef self-association 40–48 h post-transfection (25, 26), which corresponds to the end of the HIV-1 life cycle (30). We therefore explored the kinetics of WT Nef homodimer formation and membrane association at 12-h intervals using a cell-based bimolecular fluorescence complementation (BiFC) assay (31). In this approach, WT and mutant Nef coding sequences are fused to an N-terminal fragment of the YFP variant, Venus (Nef-VN), whereas complementary Nef constructs are fused to a C-terminal Venus fragment (Nef-VC). Co-expression of the Nef-VN and Nef-VC fusion proteins in the same cell results in protein–protein interaction between Nef molecules, leading to complementation of the Venus fluorophore and a bright fluorescent signal.

Cultures of 293T cells were transfected with Nef-VN and Nef-VC expression vectors (WT or the dimerization interface mutants L112A, L112D, Y115D, and F121A) and fixed with paraformaldehyde 12, 24, 36, and 48 h later. The cells were then immunostained to confirm Nef protein expression, allowing

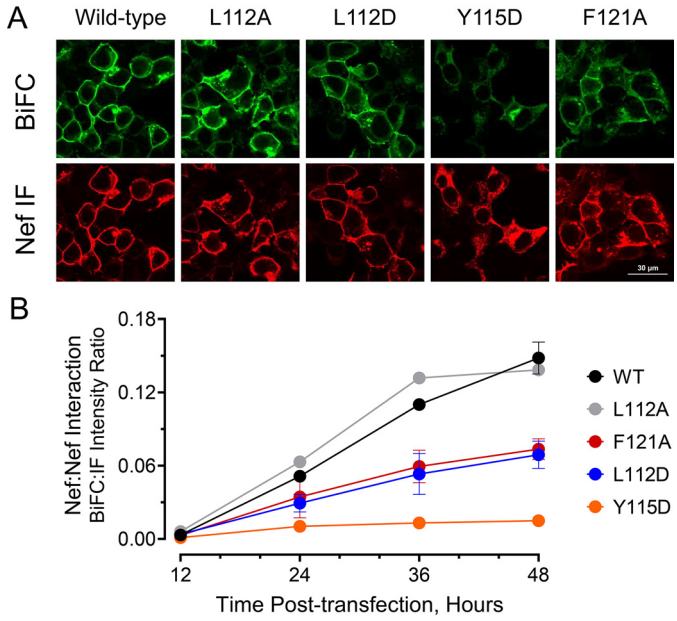

Figure 2. BiFC analysis of self-association kinetics of WT Nef and dimerization interface mutants. 293T cells were co-transfected with expression plasmids for WT and mutant Nef proteins fused to nonfluorescent complementary fragments of the YFP variant, Venus. The cells were fixed 12, 24, 36, and 48 h post-transfection and immunostained for Nef expression prior to imaging via confocal microscopy. Nef homodimerization results in reconstitution of the Venus fluorophore. *A*, representative images comparing self-association of WT and mutant Nef proteins (BiFC; *green*). Nef immunofluorescence (*IF*) is shown in *red*. *B*, time course of Nef dimerization by BiFC assay. The mean fluorescence intensity ratios of the BiFC and Nef immunofluorescence signals were calculated from a minimum of 100 cells for each condition using ImageJ. The entire experiment was repeated in duplicate, and each data point represents the mean ratio ± S.D. Complete data and statistical analysis for representative cell populations at all time points are shown in Fig. S1.

normalization of the resulting BiFC signal to Nef expression levels within each culture. Fig. 2*A* shows representative confocal images of Nef BiFC (homodimer formation) and immunofluorescence (Nef protein expression) at the 48-h end point of the experiment, whereas Nef BiFC to immunofluorescence intensity ratios across all four time points are plotted in Fig. 2*B*. Little fluorescence complementation was observed with any of the Nef BiFC pairs at 12 h, which likely reflects the low levels of Nef expression at this time point. After 24 h, WT Nef self-association was readily observed and increased in a linear fashion over 48 h. In contrast to WT Nef, the L112D, Y115D, and F121A mutants demonstrated statistically significant defects in Nef homodimerization across all time points (Fig. S1). The Y115D mutant showed the lowest ratios at each time point, with the L112D and F121A mutants exhibiting an intermediate phenotype. By contrast, the L112A mutation did not decrease the BiFC signal, suggesting that substitution of leucine with alanine does not disrupt homodimer formation. Inspection of the BiFC and immunofluorescence images suggests that all four Nef mutants remained associated with the plasma membrane, although the Y115D mutant showed increased cytoplasmic localization.

Dimerization-defective Nef attenuates HIV-1 infectivity and impairs SERINC5 antagonism

To test the requirement for Nef homodimers in SERINC5 antagonism, we first validated a 293T producer cell system to assess virion incorporation of SERINC5 and impact on viral infectivity. For these studies, 293T cells were transfected with proviral plasmids encoding WT HIV-1 or a mutant that fails to express Nef (ΔNef) in the presence and absence of a SERINC5 expression vector. Newly synthesized virions were concentrated from the culture supernatant 2 days later, and levels of virion-incorporated SERINC5 were analyzed via immunoblot. The infectivity of each viral supernatant was assessed in parallel using the TZM-bl reporter cell line (32). Expression of SERINC5 in 293T producer cells inhibited HIV-1 ΔNef infectivity but had little impact on the infectivity of the WT virus, consistent with previous results (Fig. 3*A*) (21, 22). Nef antagonism of SERINC5 within this system is consistent with levels of virion-incorporated SERINC5 observed by immunoblot, with WT virions exhibiting decreased levels of SERINC5 compared with the ΔNef virions (Fig. 3*B*). Co-transfection of an expression plasmid encoding Nef along with SERINC5 and the ΔNef proviral plasmid rescued infectivity (Fig. 3*C*) and promoted exclusion of SERINC5 from newly synthesized virions (Fig. 3*D*). These observations validate the use of the 293T producer cell system to explore the role of Nef homodimerization in SERINC5-mediated restriction of HIV-1 infectivity.

We next transfected 293T cells with HIV-1 proviral DNA bearing the Nef dimerization interface mutations L112A, L112D, Y115D, and F121A in the presence and absence of the SERINC5 expression vector. The infectivity of HIV-1 expressing the L112D, Y115D, and F121A Nef mutants was reduced in the presence of SERINC5 to the levels observed with the ΔNef virus, whereas the L112A mutant exhibited a partial loss of function (Fig. 4*A*). This finding is consistent with BiFC results showing that L112A has little impact on Nef homodimer formation in this system. Immunoblot analysis confirmed that each of the Nef mutants was expressed in transfected 293T cells (Fig. 4*B*).

In a complementary set of experiments, we explored the role of Nef dimerization in SERINC5 antagonism using the Jurkat JTAg producer cell system, which expresses a relatively high level of endogenous SERINC5 like that observed in normal CD4 T cells. An isogenic Jurkat JTag cell population in which both SERINC5 alleles are inactivated by CRISPR/Cas9 was studied in parallel (21). Jurkat JTAg WT and SERINC5-knockout cells were transfected with HIV-1 proviral constructs bearing the same Nef dimerization interface mutations, along with WT and ΔNef HIV-1. The infectivity of the viruses expressing the L112D, Y115D, and F121A Nef mutants produced in WT Jurkat JTAg cells was reduced to that of the ΔNef virus, consistent with the results in 293T producer cells co-expressing SERINC5. The infectivity of these Nef mutant viruses was restored when produced in the SERINC5-knockout cells, providing evidence of a SERINC5-dependent mechanism in this T-cell line (Fig. 4*C*). WT HIV-1 produced from either of the Jurkat producer cell lines displayed similar infectivity, consistent with the ability of WT Nef to antagonize SERINC5. Infectivity of the Nef-L112A mutant virus was also less affected by the presence or absence of SERINC5, consistent with the lack of an effect of this mutation on Nef self-association in the BiFC assay. Expression of WT and mutant forms of Nef in Jurkat producer cells was verified by immunoblot analysis (Fig. 4*D*).

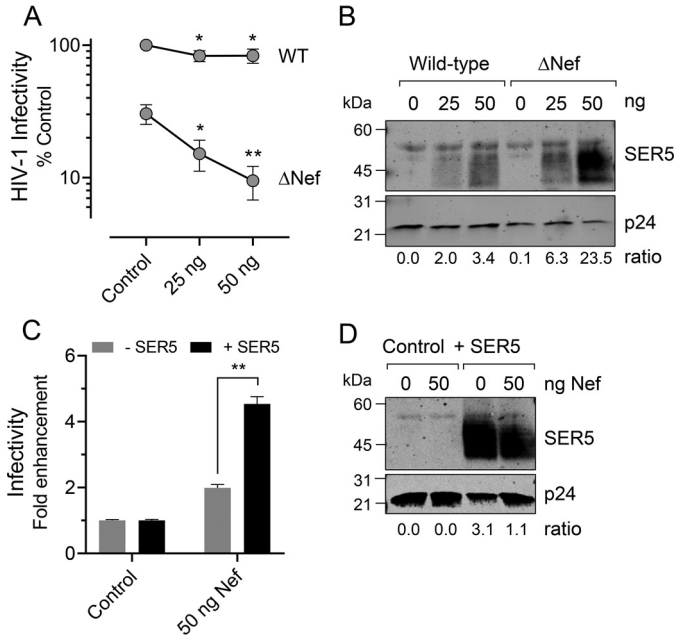

Figure 3. Nef expression antagonizes SERINC5 restriction of viral infectivity at the producer cell level. *A*, 293T cells were co-transfected with HIV-1 NL4-3 proviral plasmids competent (WT) or defective (ΔNef) for Nef expression along with 0, 25, or 50 ng of a SERINC5 expression vector. Newly released virions were harvested after 48 h, quantified via p24 AlphaLISA, and used to infect TZM-bl reporter cells. Luciferase activity was measured 48 h later and normalized to that observed with WT virus produced in the absence of SERINC5. Mean values ± S.E. are shown from three independent experiments. Significance was assessed via *t* test relative to each control. *, $p < 0.01$; **, $p < 0.001$. *B*, representative Western blots depicting incorporation of SERINC5-HA into WT and ΔNef virions. Virions were collected in parallel during the infectivity assays and purified via ultracentrifugation through a 20% sucrose cushion, lysed into sample buffer, subjected to SDS-PAGE, and immunoblotted using antibodies to p24 Gag and the HA tag on SERINC5. Band intensities were quantified using LI-COR IR imaging, and the SERINC5:p24 ratios are shown. *C*, viral antagonism of SERINC5 is rescued following ectopic expression of Nef within producer cells. The ΔNef virus was expressed in 293T cells in the presence and absence of SERINC5 and Nef expression plasmids. The data are presented as the fold enhancement of viral infectivity, defined as the ratio of infectivity between Nef-expressing and Nef-deficient producer cells. The results represent normalized mean values ± S.E. from three independent experiments. Significance was assessed via *t* test. **, $p < 0.001$. *D*, representative immunoblots displaying incorporation of SERINC5 into purified ΔNef virions produced in the presence and absence of Nef. Band intensities were quantified using LI-COR IR imaging and the SERINC5:p24 ratios are shown.

We also addressed whether Nef dimerization is important for infectivity of HIV-1 produced during a spreading infection in primary host-cell culture. SERINC5-mediated restriction has been previously observed in donor PBMCs, which also express high levels of endogenous SERINC5 (21, 22). For this experiment, PBMCs were infected with equivalent titers of WT, ΔNef, and Nef dimer mutant viruses (initially produced in 293T cells) and allowed to replicate in PBMCs for 4 days followed by infectivity assay in TZM-bl cells. As observed in the other two producer cell systems, viruses expressing the Nef L112D, Y115D, and F121A mutants showed reduced infectivity comparable with that of the ΔNef virus following amplification in PBMCs, with higher infectivity for WT and Nef-L112A HIV-1 (Fig. 4*E*).

We next investigated the requirement for Nef homodimers in the exclusion of SERINC5 from newly synthesized virions. For these experiments, 293T cells were co-transfected with HIV-1 WT, ΔNef, and Nef dimerization-defective mutant proviral DNA in the presence of the SERINC5 expression plasmids. Newly synthesized virions were isolated and incorporation of SERINC5 was assessed by immunoblotting for the C-terminal HA epitope tag (Fig. 5*A*). The amount of virus-associated SERINC5 was then normalized to p24 Gag levels from three independent experiments (Fig. 5*B*). SERINC5 incorporation into virions mirrored the infectivity data, with the L112D, Y115D, F121A, and ΔNef virions exhibiting significantly higher levels of SERINC5 than the WT and L112A viruses. These findings demonstrate that enhancement of HIV-1 infectivity requires Nef homodimers and involves a mechanism linked to antagonism of SERINC5 incorporation by Nef dimers at the producer cell level. Interestingly, HIV-1 expressing the Nef-L112D mutant showed significantly higher incorporation of SERINC5 than virus that fails to express Nef (ΔNef). As described in the following section, this effect may be due to accumulation of SERINC5 at the producer cell membrane by this mutant caused by attenuated endocytosis.

Nef homodimerization enhances SERINC5 internalization and endosomal trafficking

Previous studies have implicated Nef homodimers in CD4 down-regulation (25, 26), a process that requires the endocytic trafficking adaptor protein, AP-2. Nef-mediated antagonism of SERINC5 is also mediated by AP-2–dependent down-regulation of SERINC5 from the cell membrane, resulting in endocytosis and lysosomal degradation (22, 24). Here we demonstrate a clear increase in virion-associated SERINC5 with HIV-1 expressing dimerization-defective Nef (Fig. 5), suggesting that impaired exclusion of SERINC5 from virions expressing these Nef mutants was due to dysfunctional down-regulation of SERINC5 from the producer cell surface. To address this issue, the Jurkat SERINC5-knockout cells were transfected with expression vectors for Nef (WT or dimerization-defective mutants), which also expresses GFP as a gating marker and for SERINC5 with a hemagglutinin (HA) epitope tag on one of the extracellular loops (33). Transfected cells were then immunostained with an anti-HA antibody to detect cell-surface SERINC5 expression in the Nef-transfected (GFP+) cell population via flow cytometry. Expression of WT Nef decreased cell-surface SERINC5 expression by nearly 90% relative to the GFP-only control population. In contrast to WT Nef, the dimerization-defective mutants L112D, Y1125D, and F121A all showed significantly impaired SERINC5 down-regulation, ranging from 65 to 85% relative to the control (Fig. 6, *A* and *B*). The Nef-L112A mutant was not affected, consistent with the lack of a dimerization defect observed with this mutant. These results demonstrate that Nef homodimers are important for efficient down-regulation of SERINC5 from the cell surface.

Because of the mechanistic similarity between Nef-induced down-regulation of SERINC5 and CD4, we also explored the impact of the Nef dimer interface mutations on down-regulation of endogenous CD4 in the CEM-SS T-cell line (34). CEM-SS cells were transfected with the same Nef/GFP dual expression plasmid used for the SERINC5 study, followed by immunostaining for endogenous cell-surface CD4 and flow cytometry. Expression of

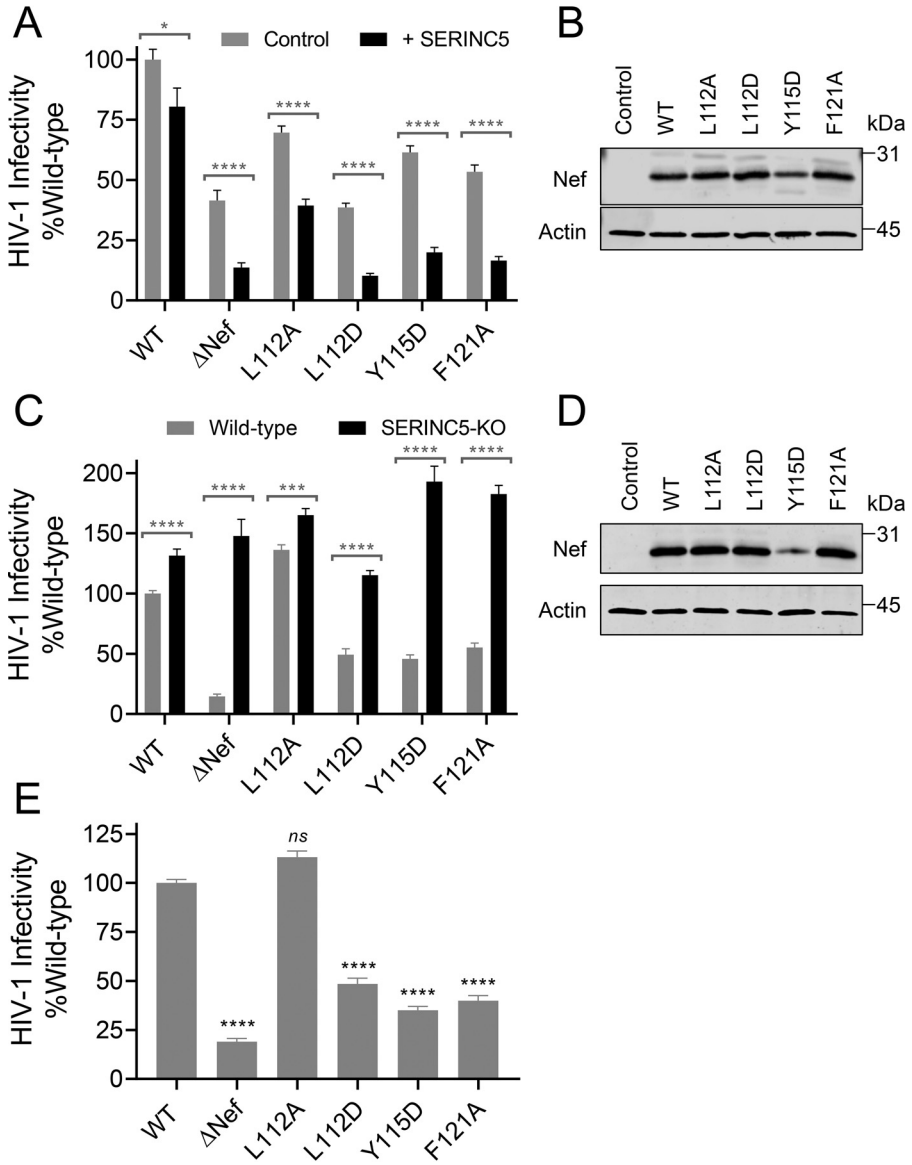

Figure 4. HIV-1 expressing dimerization-defective Nef mutants exhibit reduced infectivity. *A*, 293T cells were co-transfected with WT, ΔNef, and dimerization-defective Nef mutant (L112A, L112D, Y115D, and F121A) proviruses in the presence and absence of SERINC5, and infectivity of equivalent p24 inputs was analyzed 48 h later in TZM-bl reporter cells. Results from three independent experiments are shown normalized to the infectivity of WT virus produced in the absence of SERINC5 (*WT Control*). Each *bar* represents the mean value ± S.E. *B*, representative immunoblots verifying expression of WT and dimerization-defective Nef mutants in lysates of transfected 293T cells. Actin blots are shown as a loading control. *C*, WT and SERINC5-knockout Jurkat TAg T cells were transfected with WT, ΔNef, and dimerization-defective Nef mutant proviruses. Infectivity of equivalent p24 inputs was analyzed 48 h later in TZM-bl reporter cells. Results from three independent experiments are shown normalized to the infectivity of WT virus produced in WT Jurkat cells, with each *bar* representing the mean value ± S.E. *D*, representative immunoblots verifying expression of WT and dimerization-defective Nef mutants in lysates of transfected Jurkat cells. Actin blots are shown as a loading control. *E*, PBMCs from uninfected donors were activated with phytohemagglutinin and IL-2 for 3 days and then infected with 150 pg p24/ml of WT, ΔNef, and Nef dimerization-defective mutant viruses for 4 days. Infectivity of equivalent p24 inputs of the resulting viral supernatants were analyzed 48 h later in TZM-bl reporter cells. Results from three independent experiments are shown normalized to the infectivity of WT virus, with each *bar* representing the mean value ± S.E. In *A* and *C*, statistical significance was assessed between the indicated pairs of values by *t* test, whereas in *E* each comparison was made *versus* the WT control. *, $p < 0.05$; ***, $p < 0.001$; ****, $p < 0.0001$; *ns*, not significant.

WT Nef reduced cell-surface CD4 expression by more than 60%, whereas the L112D, Y115D, and F121A Nef mutants were completely defective for CD4 downmodulation (Fig. 7, *A* and *B*). Cells expressing Nef-L112A exhibited an intermediate phenotype, with an ~30% reduction in cell-surface CD4 expression. Although the L112A mutant does not show a decrease in homodimer formation by BiFC assay, alteration of the dimer interface by this mutation may impact the efficiency of CD4 down-regulation. Overall, these results agree with those observed with SERINC5 and are consistent with the shared mechanism of action involving AP-2–dependent endocytosis.

Following Nef-mediated endocytosis, SERINC5 traffics through Rab7+ late endosomes en route to proteolytic destruction following lysosomal fusion (21, 24). We therefore investigated whether mutations disrupting Nef dimerization also impact the intracellular trafficking of SERINC5 along this pathway. SERINC5-knockout Jurkat cells were transfected with SERINC5 fused to the mCherry fluorescent protein in

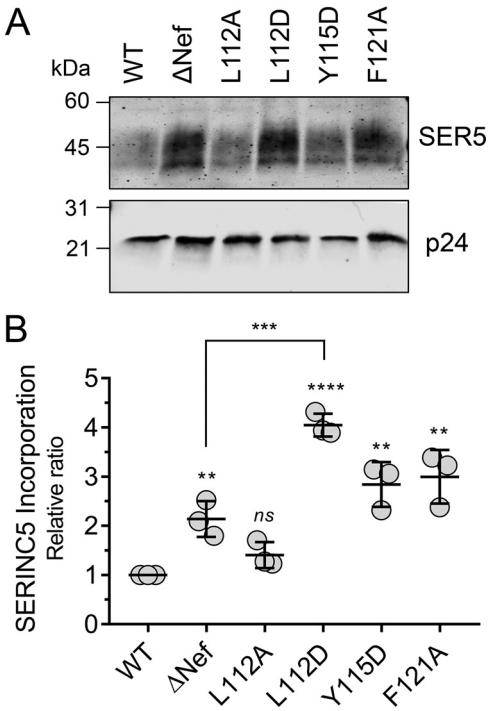

Figure 5. Dimerization-defective Nef mutants display attenuated exclusion of SERINC5 from newly synthesized virions. 293T cells were co-transfected with WT, ΔNef, and Nef dimerization interface mutant proviruses (L112A, L112D, Y115D, and F121A) in the presence of a SERINC5-HA expression vector. Newly synthesized virions were purified by ultracentrifugation through a 20% sucrose cushion, and SERINC5 incorporation was analyzed via immunoblotting along with p24 Gag as a control. *A*, representative SERINC5 and p24 immunoblots. *B*, SERINC5 and p24 protein expression levels were quantified by LI-COR Odyssey image analysis, and each data point represents the SERINC5 to p24 expression ratio for three independent experiments. Mean values in each group are indicated by the *horizontal bar* ± S.E. Statistical significance relative to WT was determined by Student's *t* test. **, $p \leq 0.01$; ****, $p \leq 0.0001$; *ns*, not significant. Note that Nef-L112D also incorporated significantly more SERINC5 than ΔNef. ***, $p \leq 0.001$.

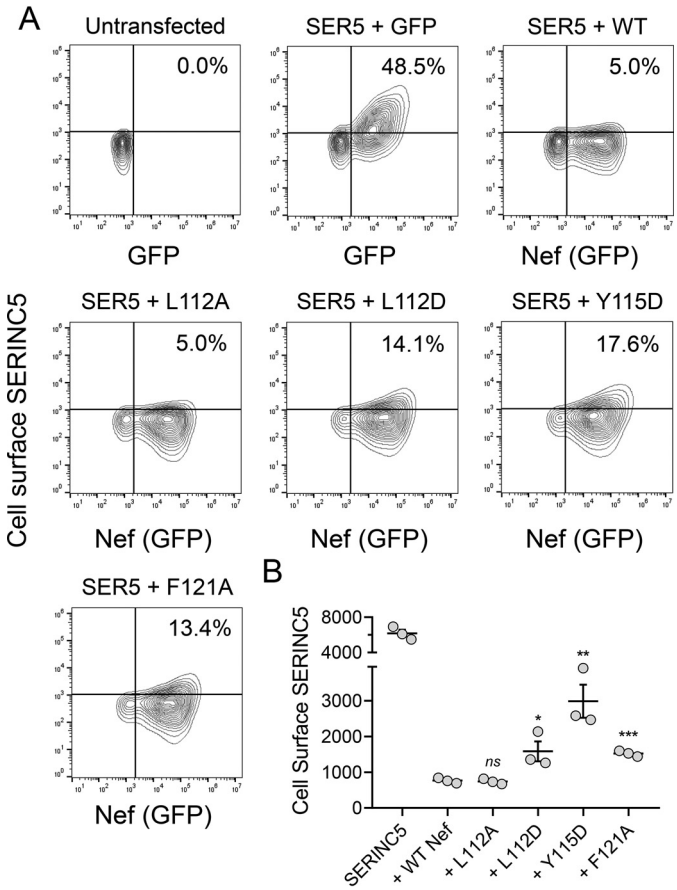

Figure 6. Nef dimerization is important for SERINC5 down-regulation. SERINC5-knockout Jurkat T cells were transfected with a dual promoter plasmid expressing WT or dimerization-defective Nef mutants, as well as GFP as a gating marker. A second plasmid was included for expression of SERINC5 tagged with an extracellular HA epitope (SERINC5-iHA). 48 h after transfection, the cells were immunostained with an HA antibody, and cell-surface expression of SERINC5-iHA was quantified via flow cytometry. *A*, representative flow cytometry plots showing impaired down-regulation of SERINC5 by Nef dimer mutants. The cells were gated on the untransfected cell population, and the percentages of SERINC5-positive and GFP-positive (marker for Nef expression) cells are indicated. *B*, levels of cell-surface SERINC5 were estimated from the SERINC5 mean fluorescence intensity within the GFP-positive cell populations from three independent experiments. Mean values in each group are indicated by the *horizontal bar* ± S.E. Statistical significance relative to WT Nef was determined by Student's *t* test. *, $p \leq 0.05$; **, $p \leq 0.01$; ***, $p < 0.001$; *ns*, not significant.

combination with WT or dimerization-defective forms of Nef fused to YFP. 2 days later, transfected cells were immunostained for the late endosomal marker, Rab7. The expression and subcellular localization of SERINC5-mCherry, Nef-YFP, and Rab7 were then analyzed via confocal microscopy. When expressed alone, SERINC5-mCherry localized almost entirely to the plasma membrane with very little co-localization with Rab7 (confocal images of representative cells are shown in Fig. 8). Co-expression of WT Nef-YFP resulted in a dramatic shift in SERINC5-mCherry localization from the cell surface into the Rab7+ endosomal compartment, observed as the co-localization of SERINC5-mCherry, Nef-YFP, and Rab7 fluorescence within multiple intracellular puncta. In marked contrast, the Nef dimer interface mutants L112D, Y115D, and F121A all showed reduced intracellular targeting of SERINC5-mCherry, with both proteins retaining co-localization to the plasma membrane. Very few intracellular Rab7+ endosomes were observed with these three Nef mutants, consistent with a defect in endocytosis and intracellular trafficking. On the other hand, the Nef-L112A mutant displayed an intermediate phenotype, co-localizing with SERINC5-mCherry at the plasma membrane and in Rab7+ endosomes.

To quantify the extent of co-localization, Pearson's correlations were calculated for co-localization of the SERINC5-mCherry and Rab7 fluorescence for a minimum of 18 individual cells (Fig. 9*A*). In the absence of Nef, the average Pearson's correlation coefficient was ~0.1, indicating little correlation in terms of subcellular localization and consistent with the lack of SERINC5 internalization in the absence of Nef. Co-expression of Nef resulted in a significant increase in the correlation coefficient (mean $\sigma > 0.5$), consistent with the observed trafficking of SERINC5 to late endosomes. The correlation coefficient was significantly reduced with all four dimerization-defective Nef mutants compared with WT Nef, consistent with the confocal images showing retention of SERINC5-mCherry at the plasma membrane. As a control, we also performed correlation analysis for the co-localization of Nef-YFP and SERINC5-mCherry fluorescence (Fig. 9*B*). Notably, no significant difference was

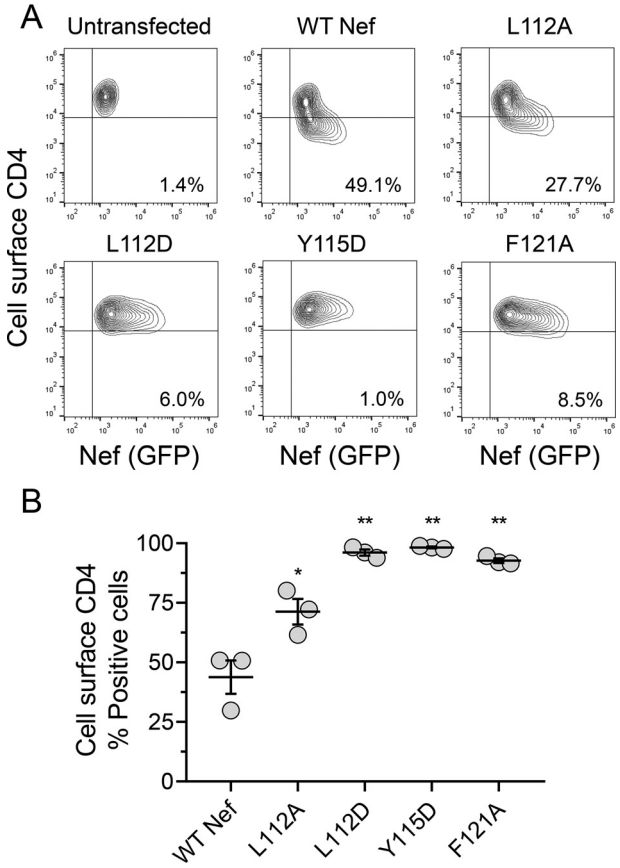

Figure 7. Nef dimerization is important for CD4 down-regulation. CEM-SS cells were transfected with a dual promoter plasmid expressing WT or dimerization-defective Nef mutants as well as GFP as a gating marker. 48 h after transfection, the cells were immunostained with a CD4 antibody and cell-surface CD4 expression was quantified via flow cytometry. *A*, representative flow cytometry plots showing impaired down-regulation of CD4 by Nef dimer mutants. The cells were gated on the untransfected CD4-positive cell population, and the percentage of Nef-expressing cells demonstrating down-regulation of CD4 from the cell surface (CD4-negative and GFP-positive) is indicated for each condition. *B*, CD4 cell-surface expression normalized to surface CD4 expression in the absence of Nef (untransfected) for three independent determinations. Mean values in each group are indicated by the *horizontal bar* ± S.E. Statistical significance relative to WT Nef was determined by Student's *t* test. *, $p \leq 0.05$; **, $p \leq 0.01$).

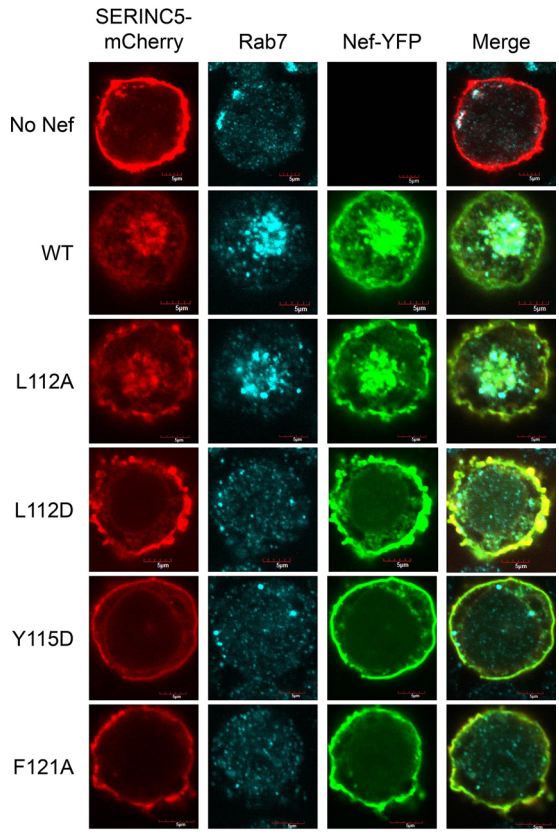

Figure 8. Nef dimerization is important for internalization of SERINC5. SERINC5-knockout Jurkat T cells were co-transfected with expression plasmids for SERINC5-mCherry together with WT or dimerization-defective Nef mutants fused to YFP or with the empty vector as a control. 48 h later, the cells were fixed, permeabilized, and stained with an antibody to the late endosomal marker Rab7. Representative single-cell images of SERINC5-mCherry (*red*), Nef-YFP (*green*), and Rab7 fluorescence are shown along with a merged image. *Scale bar*, 5 μM.

observed in these co-localization correlations (mean $\sigma \approx 0.9$ in each case), hinting that the Nef dimer mutations may not affect interaction of Nef with SERINC5. This possibility was explored directly using BiFC as described in the next section.

Disruption of Nef homodimerization does not impair interaction with SERINC5 or AP-2

Previous work suggests that Nef and SERINC5 interact directly within cells, with Nef-mediated antagonism of SERINC5 mediated by a large intracellular loop within SERINC5 (24, 35). Although an X-ray crystal structure of SERINC5 has been elucidated recently (36), electron density for this intracellular loop was not observed, suggesting that it is unstructured. Furthermore, the specific region of Nef responsible for interaction with SERINC5 is not known. Although the data presented above support a role for Nef homodimers in SERINC5 down-regulation, the possibility remains that the amino acids involved in Nef homodimer formation may also contribute to interaction with SERINC5. To test this possibility, we employed the BiFC assay to visualize and quantify direct interaction of Nef with SERINC5 in cells (24).

SERINC5-VN and each of the Nef-VC fusion proteins (WT and mutants) were co-expressed in 293T cells followed by immunostaining for Nef and SERINC5 (via the HA tag) to control for protein expression levels. As a negative control, we also included a mutant of Nef that cannot be myristoylated (Nef-G2A) and therefore exhibits impaired membrane localization and SERINC5 interaction (24). Co-expression of WT Nef-VC with SERINC5-VN resulted in a positive BiFC signal, supporting direct protein–protein interaction in cells (Fig. 10*A*). Immunofluorescence for both Nef and SERINC5 expression was also readily observed in the same cells and co-localizes with the BiFC signal (Fig. S2). All four Nef-VC dimer interface mutants also generated a BiFC signal when partnered with SERINC5-VN, whereas the Nef-G2A mutant resulted in a lower BiFC signal despite a similar level of expression as WT Nef based on immunofluorescence. To quantify these results, the fluorescence intensity for the BiFC signal of each Nef interaction with SERINC5 was normalized to Nef expression levels as determined by immunofluorescence, and the resulting fluorescence intensity ratios are plotted for at least 100 cells in Fig. 10*B*. No significant difference in SERINC5 interaction was observed between

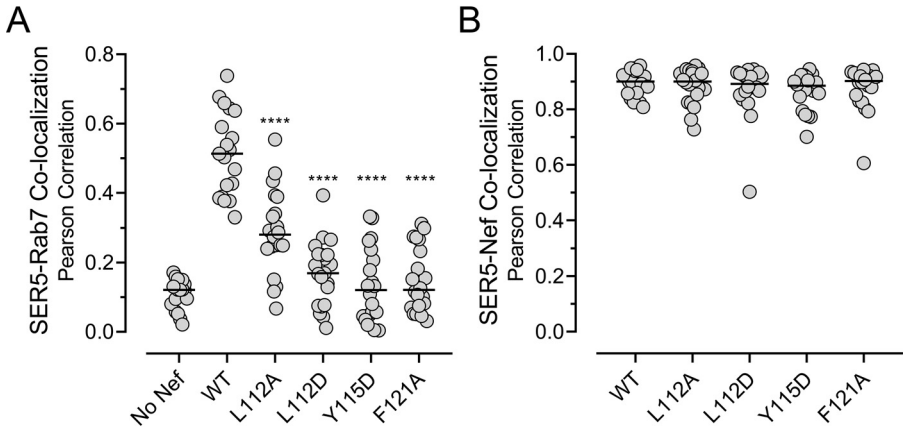

Figure 9. Disruption of Nef dimerization impairs internalization and trafficking of SERINC5-mCherry to Rab7+ endosomes. SERINC5-knockout Jurkat T cells were co-transfected with expression plasmids expressing SERINC5-mCherry together with WT or dimerization-defective Nef mutants fused to YFP and immunostained with an antibody to the late endosomal marker Rab7 as described in the legend to Fig. 8. *A*, single-cell confocal images were subjected to Pearson's correlation coefficient analysis to quantify the extent of SERINC5-mCherry co-localization with Rab7. A minimum of 18–20 cells/condition were analyzed across three independent experiments, and the Pearson's correlation coefficient for each cell is shown with the median value indicated by the *horizontal bar*. Statistical significance among the groups was performed via one-way ANOVA with Dunnett's multiple comparisons test relative to the cell population expressing WT Nef. ****, $p \leq 0.0001$. *B*, Pearson's correlation analysis of SERINC5-mCherry co-localization with Nef-YFP was performed in the same groups of cells, with median correlation coefficients indicated by the *horizontal bars*. Statistical analysis via ordinary one-way ANOVA did not reveal significant differences between the groups.

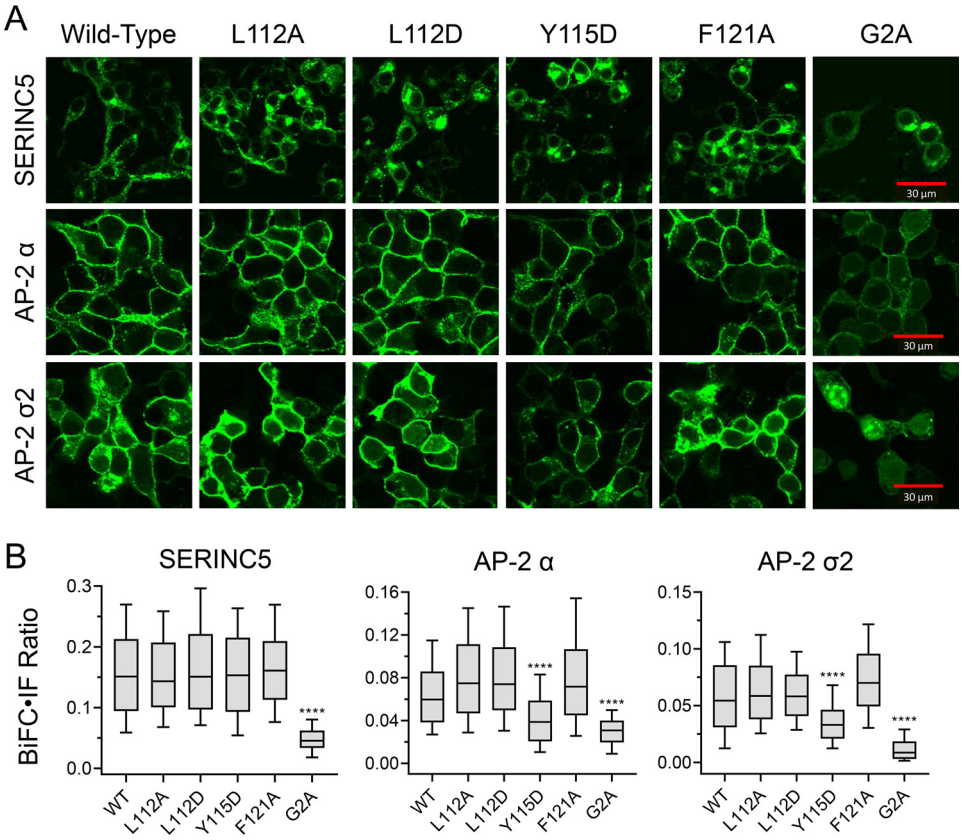

Figure 10. Nef dimerization is not required for interaction with SERINC5 or AP-2. 293T cells were co-transfected with expression plasmids for SERINC5, AP-2α, or AP-2 σ2 fused to an N-terminal fragment of Venus along with WT Nef, the dimerization-interface mutants (L112A, L112D, Y115D, and F121A) or myristylation-defective Nef (G2A) fused to the complementary C-terminal Venus fragment. The cells were fixed, permeabilized, and immunostained 48 h later for Nef and either SERINC5 or the AP-2 subunits prior to confocal microscopy. *A*, representative BiFC images showing interaction of each Nef protein with SERINC5 (*upper row*), AP-2α (*middle row*), and AP-2 σ2 (*bottom row*). *B*, the mean fluorescence intensities of BiFC and Nef immunofluorescence were calculated for a minimum of 100 cells within each pair using ImageJ. The distribution of BiFC:immunofluorescence ratios for each cell population are plotted as box-and-whisker plots with the *boxes* showing the 25th to 75th percentiles and the *whiskers* showing the 10th to 90th percentiles. Statistical analysis was performed via one-way ANOVA with Dunnett's multiple comparisons test relative to the cell population expression WT Nef. ****, $p \leq 0.0001$ (all other cases not significant).

WT Nef and the dimerization-defective mutants, demonstrating that disruption of the Nef homodimerization interface does not affect interaction with SERINC5. In contrast, the Nef-G2A mutant showed a significant decrease in SERINC5 interaction, consistent with the inability of this mutant to localize to the plasma membrane. These observations suggest that impaired antagonism of SERINC5 by the Nef dimer mutants is not due to a defect in SERINC5 interaction with Nef.

Down-regulation of SERINC5 by Nef also requires interaction with AP-2 through a complex of its α and σ2 subunits (19), resulting in endocytosis and lysosomal degradation. The structural alignment described above shows that the dimer interface of Nef does not overlap with regions of AP-2 contact, which involve a distinct intracellular loop in the Nef core (Fig. 1*B*). To determine whether Nef dimer interface mutations affect AP-2 subunit interaction, we employed a similar BiFC approach in which each Nef protein was fused to the N-terminal fragment of Venus (Nef-VN), whereas the AP-2 α and σ2 subunits were fused to the C-terminal fragment (α-VC and σ2-VC). The AP-2 fusion proteins also included a V5 tag for immunofluorescence detection as described previously (25). Each AP-2–VC construct was co-expressed with the WT and mutant forms of Nef-VN in 293T cells, followed by immunofluorescence detection of protein expression and confocal microscopy. WT Nef as well as the dimer interface mutants all exhibited membrane-localized BiFC signals when co-expressed with AP-2 α-VC or σ2-VC (Fig. 10*A*). We then calculated normalized BiFC interaction ratios for Nef with each AP-2 subunit as described above for SERINC5 (Fig. 10*B*). The Nef L112A, L112D, and F121A mutants interacted with each AP-2 subunit to the same extent as WT Nef, whereas the Y115D mutant ratio was somewhat reduced despite membrane localization. The Nef-G2A mutant showed a significant loss of interaction with both AP-2 subunits, consistent with its inability to localize to the plasma membrane. Expression of each Nef and AP-2 protein was confirmed by immunofluorescence microscopy, and representative images are presented in Figs. S3 and S4. These experiments show that amino acids present in the Nef dimer interface, except for Tyr^{115}, are not involved in AP-2 interaction at the cell membrane.

Discussion

Antagonism of the host cell restriction factor SERINC5 is a key mechanism by which Nef promotes HIV-1 infectivity. Nef triggers internalization of SERINC5 from the surface of infected cells, thereby preventing incorporation of SERINC5 into budding virions and subsequent impairment of viral entry (21, 22). Although the cellular mechanisms of Nef-mediated SERINC5 internalization and degradation have been established, little is known about the structural features of Nef required for SERINC5 engagement and association with AP-2 for down-regulation. In this study, we assessed the function of dimerization defective Nef mutants across all stages of SERINC5 antagonism including viral infectivity, virion incorporation of SERINC5, down-regulation of SERINC5 from the surface of producer cells, and the intracellular fate of SERINC5. We observed consistent impairment of all stages of SERINC5 antagonism with three distinct dimerization defective Nef mutants, demonstrating that Nef counteracts SERINC5 as a homodimer. Importantly, each dimerization-defective Nef mutant retained interaction with both SERINC5 and the AP-2 subunits required for internalization, supporting the idea that the Nef homodimer may act as a bridge to link SERINC5 to the AP-2 pathway as illustrated in Fig. 11.

Our data show that Nef dimerization promotes the infectivity of newly synthesized HIV-1 particles produced by transfected 293T cells, as well as a T-cell line, in a SERINC5-dependent manner. These results may provide a mechanistic explanation for previous studies in which similar mutations were shown to influence viral infectivity. For example, substitution of Nef amino acids Leu^{112} and Phe^{121} has been reported to negatively impact HIV-1 infectivity and replication (37), although the role of SERINC5 was not known at that time. These same residues have also been linked to Nef recruitment of the endocytic GTPase Dynamin-2, as well as the human peroxisomal thioesterase 8 (37, 38), suggesting a role for Nef homodimers in these interactions as well.

We observed that Nef-defective HIV-1 (ΔNef virus) produced in 293T cells in the absence of SERINC5 co-expression was less infectious than WT HIV-1 (Fig. 4*A*). This finding suggests that 293T cells may express an endogenous Nef-sensitive restriction factor unrelated to SERINC5. Wu *et al.* (39) also reported the existence of an unidentified, Nef-sensitive restriction factor other than SERINC5. In our study, this additional factor appears to be limited to 293T cells, because WT and ΔNef HIV-1 produced from SERINC5-knockout Jurkat T cells showed equivalent infectivity.

Nef dimerization enhances SERINC5 down-regulation from the cell surface, which is mechanistically like Nef-dependent down-regulation of CD4. Both SERINC5 and CD4 down-regulation are mediated via AP-2 and clathrin-dependent endocytosis. Mutations that disrupt Nef myristoylation and membrane association (G2A), as well as the dileucine motif required for AP-2 recruitment (L164A,L165A), impair down-regulation of both proteins (21, 40, 41). Nef dimerization-defective mutants impaired for down-regulation of SERINC5 were also unable to down-regulate CD4. Expression of WT Nef in Jurkat T cells led to the relocalization of SERINC5 from the cell membrane into intracellular Rab7+ compartments (24), a fate also shared by CD4 (42). Intracellular trafficking and Rab7 co-localization were also significantly disrupted by mutations in the Nef dimerization interface. These findings suggest that Nef homodimers may link both SERINC5 and CD4 to the AP-2 endocytic pathway through separate binding surfaces on each Nef monomer (Fig. 11).

BiFC assays presented here demonstrate direct Nef–SERINC5 interaction at the plasma membrane in cells, consistent with recent work (24, 43). Importantly, mutations in residues essential for Nef homodimer formation do not impact interaction of Nef with SERINC5 in the BiFC assay, consistent with a role for the Nef αB helix in homodimer formation as demonstrated by X-ray crystal structures (27, 28) rather than interaction with signaling partners. Although the mechanism of SERINC5 engagement by Nef remains enigmatic, recent studies have illuminated the regions of SERINC5 required for viral restriction and susceptibility to Nef antagonism (36). SERINC5

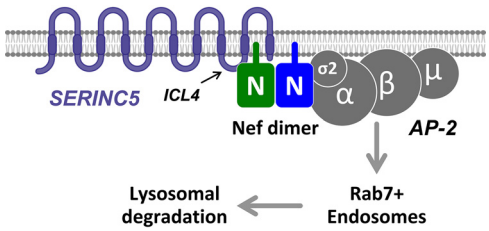

Figure 11. Hypothetical model of SERINC5 interaction and down-regulation by HIV-1 Nef homodimers via AP-2–mediated endocytosis. Myristoylated Nef associates with the host-cell membrane and forms homodimers, allowing for simultaneous recruitment of AP-2 and SERINC5 through intracellular loop 4 (*ICL4*). The resulting SERINC5–Nef–AP-2 complex drives down-regulation of SERINC5 from the cell membrane, thereby excluding it from budding virions. The complex traffics through Rab7$^+$ late endosomes, leading to lysosomal degradation.

is an integral membrane protein with ten transmembrane helices and four intracellular loops (36). Sensitivity of SERINC5 to Nef antagonism appears to map to the fourth intracellular loop, because deletion or replacement of this loop with the Nef-resistant SERINC2 counterpart renders SERINC5 immune to Nef down-regulation (35). However, whether this loop is the sole point of contact in the Nef–SERINC5 complex remains an important open question.

The SERINC5-binding site within Nef also remains elusive. A recent structural study of SIVmm Nef in complex with AP-2 and tetherin showed that mutation of a critical residue within the tetherin-binding site (His^{196}) also impairs antagonism of SERINC5, suggesting a shared binding mechanism (41). In HIV-1 Nef, the analogous residue (His^{166}) is in the flexible internal loop adjacent to the dileucine motif essential for AP-2 σ2 engagement. This Nef region is separate from the αB helix involved in self-association (Fig. 1*C*), consistent with the idea that Nef binds SERINC5 as a dimer. Nevertheless, a direct role for this binding site in HIV-1 Nef SERINC5 association remains to be confirmed.

Although the binding site for SERINC5 within Nef remains to be identified, our BiFC data clearly show that conserved residues in the dimer interface are not required for SERINC5 engagement. Nef dimer interface mutants L112A, L112D, and F121A also retained interaction with the AP-2 α and σ2 subunits via BiFC, consistent with the distinct interfaces for homodimerization and AP-2 recruitment illustrated by structural alignment in Fig. 1*C*. However, the Nef Y115D mutant demonstrated statistically lower association with both AP-2 subunits. Although the Y115D mutation may impact Nef folding or overall stability, unimpaired interaction of this mutant with SERINC5 suggests otherwise. Another possibility is that Tyr^{115} may have an allosteric influence on AP-2 binding by Nef.

In summary, disruption of Nef dimerization attenuates SERINC5 antagonism without impairing recruitment of SERINC5 or AP-2 as required for internalization. Although the protein dynamics controlling Nef-dependent SERINC5 down-regulation remain a mystery, our data support a mechanism in which Nef homodimers promote Nef–SERINC5–AP-2 complex formation at some point prior to SERINC5 internalization. One Nef monomer within the dimer may contact SERINC5, whereas the other engages AP-2, with the Nef dimer interface bridging the two proteins to initiate clathrin-mediated endocytosis. Understanding the molecular determinants of SERINC5 antagonism by Nef may help to identify therapeutic strategies that promote SERINC5 virion incorporation and restriction of viral infectivity. Along these lines, docking studies of small molecule inhibitors of Nef-mediated enhancement of viral infectivity have identified potential binding sites within the dimer interface (12, 44, 45). Disruption of the Nef homodimer by these compounds may explain their inhibitory effects on multiple Nef functions, including not only infectivity but also host-cell kinase activation, receptor down-regulation, and enhancement of viral replication. Thus, the homodimer interface represents an attractive target for new antiretroviral drug development targeting Nef.

Experimental procedures

Cell culture

The human embryonic kidney cell line 293T was purchased from the ATCC. TZM-bl reporter cells were obtained from the AIDS Research and Reference Reagent Program. Both cell lines were grown in Dulbecco's modified Eagle's medium supplemented with 10% fetal bovine serum (Gemini Bio-Products). Jurkat JTAg T cells (WT and SERINC5-knockout) were a kind gift from Dr. Massimo Pizzato, University of Trento, whereas the CEM-SS T-cell line was kindly provided by Dr. Mark Brockman, Simon Fraser University. Both T-cell lines were cultured in RPMI 1640 medium supplemented with 10% fetal bovine serum, L-glutamine, and 2 μg/ml puromycin (CEM-SS cells only). Donor PBMCs were obtained from Vitalant Pittsburgh, isolated by Ficoll gradient centrifugation, and activated for 3 days with phytohemagglutinin (Sigma, catalog no. L1668) and IL-2 (Thermo Fisher, catalog no. CB-40043B) as described elsewhere (44).

Antibodies

Primary antibodies were obtained from the AIDS Research and Reference Reagent Program (anti-p24, catalog no. 4121; anti-Nef polyclonal, catalog no. 2949; anti-Nef 6.2, catalog no. 153) and purchased from Sigma–Aldrich (anti-HA, catalog no. H6908), Millipore (anti-actin, catalog no. Mab1501R; anti-V5, catalog no. AB3702), BD (anti-CD4-phycoerythrin, catalog no. 55534), Biolegend (HA.11-647, catalog no. 16B12), and Santa Cruz (anti-Rab7, catalog no. B-3). Secondary antibodies were purchased from LICOR (IRDye 680LT donkey anti-mouse, catalog no. 926-68022; IRDye 800CW donkey anti-rabbit, catalog no. 926-32213), Thermo Fisher (anti-mouse Alexa Fluor647, catalog no. A-21236), Invitrogen (anti-rabbit Pacific Blue, catalog no. P-10994), and Southern Biotech (anti-mouse Texas Red, catalog no. 1031-07; anti-rabbit Texas Red, catalog no. 4050-7).

Plasmids

Construction of the pUC18 HIV-1 NL4-3/SF2Nef proviral plasmid is described elsewhere (46). The Nef dimer interface mutations (L112A, L112D, Y115D, and F121A) were introduced into the pUC18 NL4-3/SF2Nef and pcDNA3.1 Nef-Venus (11) constructs via the Agilent II XL site-directed

mutagenesis kit. Expression vectors for SERINC5 (pBJ5-SERINC5-HA and pBJ5-SERINC5-iHA) were a kind gift from Dr. Heinrich Göttlinger (University of Massachusetts Medical School). The pSELECT-zeoGFP-based expression plasmids for WT and dimer interface mutants of Nef have been previously described (11). SERINC5-mCherry was purchased from GeneCopoeia. The pcDNA3.1 SERINC5-VN-HA construct for BiFC was the kind gift of Dr. Yong-Hui Zheng, Michigan State University. Construction of BiFC expression plasmids for AP-2 subunits in pcDNA3.1 (σ2-V5-VC and α-V5-VC), as well as pcDNA3.1 Nef-YFP, have been previously reported (25).

HIV-1 replication and infectivity assays

Human 293T cells were transfected with proviral expression plasmids using Xtreme Gene 9 (Sigma–Aldrich) for 48 h prior to harvesting the viral supernatant. Jurkat JTAg WT and SERINC5-knockout cells were transfected with proviral plasmids using the Amaxa cell line nucleofector kit V, and the resulting viral supernatant was harvested 48 h later. PBMCs were infected with 150 pg/ml of HIV-1 (WT, ΔNef, and Nef mutants) for 4 days prior to assay. HIV-1 titers in clarified supernatants from all producer cells were quantified using the PerkinElmer p24 AlphaLISA detection Kit. Each viral supernatant (5,000 pg/ml p24) was then used to infect TZM-bl cells in 96-well plates (2.5×10^4 cells/well). After 48 h, the cells were lysed in Promega luciferase buffer, transferred to a white 96-well plate, mixed with luciferase reagent, and measured using a Biotek Cytation 5 plate reader.

SERINC5 incorporation assay

Viral supernatants from 293T cells co-transfected with proviral DNA and the SERINC5-HA expression plasmid pBJ5-SERINC5-HA were clarified by centrifugation and HIV-1 virions were purified through a 20% sucrose cushion at 100,000 × *g* for 1 h at 4 °C. The supernatant was carefully removed, and virions were lysed directly in SDS-PAGE sample buffer (100 mM Tris-HCl, pH 6.8, 5 mM tris(2-carboxyethyl)phosphine hydrochloride, 10% glycerol, 4% SDS). The viral lysates were heated to 37 °C for 15 min, resolved on 4–20% SDS-PAGE gradient gels, transferred to nitrocellulose membranes, and incubated overnight at 4 °C with primary antibodies to HIV-1 p24 (1:1000) or the HA tag on SERINC5 (1:500). The blots were washed with TBS with 0.1% Tween-20 (TBST) and then incubated for 2 h with LI-COR IR-Dye secondary antibodies (1:10,000). The blots were imaged using the LI-COR Odyssey IR imaging system and the LI-COR ImageStudio Lite software.

Immunoblotting

Jurkat and 293T producer cells were lysed 48 h post-transfection with radioimmune precipitation assay buffer (50 mM Tris-HCl, pH 7.4, 150 mM NaCl, 1 mM EDTA, 1% Triton X-100, 0.1% SDS, 1% sodium deoxycholate) supplemented with protease inhibitors. Lysate protein concentrations were quantified via Bradford assay (Bio-Rad Bradford reagent) and normalized to 50 μg/ml. Lysate aliquots were heated in SDS-PAGE sample buffer at 95 °C for 10 min, resolved on 12% SDS-PAGE gels, and transferred to nitrocellulose membranes. Immunoblots were blocked for 1 h with Superblock TBS blocking buffer (Thermo Fisher) then probed overnight at 4 °C with antibodies to Nef (anti-Nef polyclonal, catalog no. 2949, 1:500) or actin (1:5000). Following washes in TBST, the blots were incubated for 2 h with LI-COR IR-Dye secondary antibodies (1:10,000) and imaged using the LI-COR Odyssey system and software.

Flow cytometry

Jurkat SERINC5-knockout cells and CEM-SS cells were transfected with the pSELECT-GFPzeo expression vector encoding WT and mutant forms of Nef, pSELECT-GFPzeo alone, and/or pBJ-SERINC5-iHA as described above. 48 h later, the cells were washed in 1× PBS supplemented with 2% fetal bovine serum and stained for 1 h at ambient temperature with APC-conjugated anti-HA.11 (to detect SERINC5-HA) or phycoerythrin-conjugated anti-human CD4 antibody (both antibodies diluted 1:200). After washing, the cells were analyzed for GFP (to quantify Nef expression) and either HA (to quantify JTAg cell-surface S5-iHA expression) or phycoerythrin (to quantify CEM-SS cell-surface CD4 expression) using a BD Accuri flow cytometer. The data were analyzed via BD CSampler software and illustrated using the FlowJo software package.

BiFC and confocal microscopy

293T cells were plated onto 35-mm coverslip-bottom dishes (MatTek, catalog no. P35G-1.5-14-C) and allowed to attach overnight. The cells were then transfected with pcDNA3.1 expression vectors encoding complementary BiFC partners using Xtreme Gene 9. 48 h later, the cells were fixed with 4% paraformaldehyde for 10 min, permeabilized with 0.2% Triton X-100 for 15 min, and blocked with 2% BSA in PBS for 1 h. The cells were then stained overnight at 4 °C with primary antibodies directed at the V5 tag, the HA tag, or Nef (catalog no.153). Following washing, the cells were stained for 1 h with secondary antibodies conjugated to Texas Red (1:1000), Pacific Blue (1:500), or Alexa Fluor 647 (1:1000). Fluorescent images were acquired with an Olympus Fluoview FV1000 confocal microscope using the 40× objective and *x*–*y* scan mode. Immunofluorescence and BiFC signal intensities were quantified via ImageJ and are represented as the ratio of BiFC to Nef immunofluorescence as reported previously (11).

Co-localization of SERINC5 with Nef and Rab7+ endosomes was assessed in Jurkat JTAg SERINC5-knockout cells following transfection with SERINC5-mCherry and/or Nef-YFP (WT and dimer mutants) expression vectors as described above. Coverslip-bottom 35-mm dishes (MatTek) were treated with a 0.01% poly-L-lysine solution (Sigma) for 1 h at 37 °C and left to air-dry for 30 min. Transfected cells (1.2×10^6 in 200 μl of RPMI) were added to the poly-L-lysine–treated coverslips for 30 min at 37 °C. The cells were then fixed with 4% paraformaldehyde for 10 min, permeabilized with 0.2% Triton X-100 for 15 min, and blocked with 2% BSA in PBS for 1 h at room temperature. The cells were probed with a mouse monoclonal Rab7 antibody (1:1000) overnight at 4 °C and then stained with an anti-mouse Alexa Fluor 647-conjugated secondary antibody (1:1000). The cells were imaged using an Olympus Fluoview FV1000 confocal microscope with a 60× oil objective and *x*–*y*

scan mode. Pearson's correlation coefficients for co-localization were generated using the FV1000 Fluoview software.

Data availability

All data are contained within the article and the supporting information.

Acknowledgments—We thank Drs. Massimo Pizzato and Mark Brockman for providing T-cell lines and Drs. Heinrich Göttlinger and Yong-Hui Zheng for SERINC5 expression vectors.

Funding and additional information—This work was supported by National Institutes of Health Grants AI057083 and AI126617. R. P. S. was supported in part by the Pittsburgh AIDS Research Training Grant T32 AI065380 through the National Institutes of Health. The content is solely the responsibility of the authors and does not necessarily represent the official views of the National Institutes of Health.

Conflict of interest—The authors declare that they have no conflicts of interest with the contents of this article.

Abbreviations—The abbreviations used are: SIV, simian immunodeficiency virus; PBMC, peripheral blood mononuclear cell; PDB, Protein Data Bank; BiFC, bimolecular fluorescence complementation; HA, hemagglutinin; ANOVA, analysis of variance; IL, interleukin.

References

1. Laguette, N., Brégnard, C., Benichou, S., and Basmaciogullari, S. (2010) Human immunodeficiency virus (HIV) type-1, HIV-2 and simian immunodeficiency virus Nef proteins. *Mol. Aspects Med.* **31,** 418–433 CrossRef Medline
2. Hanna, Z., Kay, D. G., Rebai, N., Guimond, A., Jothy, S., and Jolicoeur, P. (1998) Nef harbors a major determinant of pathogenicity for an AIDS-like disease induced by HIV-1 in transgenic mice. *Cell* **95,** 163–175 CrossRef Medline
3. Deacon, N. J., Tsykin, A., Solomon, A., Smith, K., Ludford-Menting, M., Hooker, D. J., McPhee, D. A., Greenway, A. L., Ellett, A., Chatfield, C., Lawson, V. A., Crowe, S., Maerz, A., Sonza, S., Learmont, J., *et al.* (1995) Genomic structure of an attenuated quasi species of HIV-1 from a blood transfusion donor and recipients. *Science* **270,** 988–991 CrossRef Medline
4. Kirchhoff, F., Greenough, T. C., Brettler, D. B., Sullivan, J. L., and Desrosiers, R. C. (1995) Absence of intact nef sequences in a long-term survivor with nonprogressive HIV-1 infection. *N. Engl. J. Med* **332,** 228–232 CrossRef Medline
5. Kestier, H. W., 3rd, Ringler, D. J., Mori, K., Panicali, D. L., Sehgal, P. K., Daniel, M. D., and Desrosiers, R. C. (1991) Importance of the nef gene for maintenance of high viral loads and for development of AIDS. *Cell* **65,** 651–662 CrossRef Medline
6. Aiken, C., Konner, J., Landau, N. R., Lenburg, M. E., and Trono, D. (1994) Nef induces CD4 endocytosis: requirement for a critical dileucine motif in the membrane-proximal CD4 cytoplasmic domain. *Cell* **76,** 853–864 CrossRef Medline
7. Jäger, S., Cimermancic, P., Gulbahce, N., Johnson, J. R., McGovern, K. E., Clarke, S. C., Shales, M., Mercenne, G., Pache, L., Li, K., Hernandez, H., Jang, G. M., Roth, S. L., Akiva, E., Marlett, J., *et al.* (2011) Global landscape of HIV–human protein complexes. *Nature* **481,** 365–370 CrossRef Medline
8. Briggs, S. D., Sharkey, M., Stevenson, M., and Smithgall, T. E. (1997) SH3-mediated Hck tyrosine kinase activation and fibroblast transformation by the Nef protein of HIV-1. *J. Biol. Chem.* **272,** 17899–17902 CrossRef Medline
9. Trible, R. P., Emert-Sedlak, L., and Smithgall, T. E. (2006) HIV-1 Nef selectively activates SRC family kinases HCK, LYN, and c-SRC through direct SH3 domain interaction. *J. Biol. Chem.* **281,** 27029–27038 CrossRef Medline
10. Tarafdar, S., Poe, J. A., and Smithgall, T. E. (2014) The accessory factor Nef links HIV-1 to Tec/Btk kinases in an Src homology 3 domain–dependent manner. *J. Biol. Chem.* **289,** 15718–15728 CrossRef Medline
11. Li, W. F., Aryal, M., Shu, S. T., and Smithgall, T. E. (2020) HIV-1 Nef dimers short-circuit immune receptor signaling by activating Tec-family kinases at the host cell membrane. *J. Biol. Chem.* **295,** 5163–5174 CrossRef Medline
12. Emert-Sedlak, L. A., Narute, P., Shu, S. T., Poe, J. A., Shi, H., Yanamala, N., Alvarado, J. J., Lazo, J. S., Yeh, J. I., Johnston, P. A., and Smithgall, T. E. (2013) Effector kinase coupling enables high-throughput screens for direct HIV-1 Nef antagonists with antiretroviral activity. *Chem. Biol.* **20,** 82–91 CrossRef Medline
13. Emert-Sedlak, L., Kodama, T., Lerner, E. C., Dai, W., Foster, C., Day, B. W., Lazo, J. S., and Smithgall, T. E. (2009) Chemical library screens targeting an HIV-1 accessory factor/host cell kinase complex identify novel antiretroviral compounds. *ACS Chem. Biol.* **4,** 939–947 CrossRef Medline
14. Readinger, J. A., Schiralli, G. M., Jiang, J. K., Thomas, C. J., August, A., Henderson, A. J., and Schwartzberg, P. L. (2008) Selective targeting of ITK blocks multiple steps of HIV replication. *Proc. Natl. Acad. Sci. U.S.A.* **105,** 6684–6689 CrossRef Medline
15. Schwartz, O., Maréchal, V., Le, G. S., Lemonnier, F., and Heard, J. M. (1996) Endocytosis of major histocompatibility complex class I molecules is induced by the HIV-1 Nef protein. *Nat. Med.* **2,** 338–342 CrossRef Medline
16. Sloan, R. D., Donahue, D. A., Kuhl, B. D., Bar-Magen, T., and Wainberg, M. A. (2010) Expression of Nef from unintegrated HIV-1 DNA downregulates cell surface CXCR4 and CCR5 on T-lymphocytes. *Retrovirology* **7,** 44 CrossRef Medline
17. Pereira, E. A., and daSilva, L. L. (2016) HIV-1 Nef: taking control of protein trafficking. *Traffic* **17,** 976–996 CrossRef Medline
18. Janvier, K., Craig, H., Hitchin, D., Madrid, R., Sol-Foulon, N., Renault, L., Cherfils, J., Cassel, D., Benichou, S., and Guatelli, J. (2003) HIV-1 Nef stabilizes the association of adaptor protein complexes with membranes. *J. Biol. Chem.* **278,** 8725–8732 CrossRef Medline
19. Ren, X., Park, S. Y., Bonifacino, J. S., and Hurley, J. H. (2014) How HIV-1 Nef hijacks the AP-2 clathrin adaptor to downregulate CD4. *eLife* **3,** e01754 CrossRef Medline
20. Gondim, M. V., Wiltzer-Bach, L., Maurer, B., Banning, C., Arganaraz, E., and Schindler, M. (2015) AP-2 is the crucial clathrin adaptor protein for CD4 downmodulation by HIV-1 Nef in infected primary CD4+ T cells. *J. Virol.* **89,** 12518–12524 CrossRef Medline
21. Rosa, A., Chande, A., Ziglio, S., De, S. V., Bertorelli, R., Goh, S. L., McCauley, S. M., Nowosielska, A., Antonarakis, S. E., Luban, J., Santoni, F. A., and Pizzato, M. (2015) HIV-1 Nef promotes infection by excluding SERINC5 from virion incorporation. *Nature* **526,** 212–217 CrossRef Medline
22. Usami, Y., Wu, Y., and Göttlinger, H. G. (2015) SERINC3 and SERINC5 restrict HIV-1 infectivity and are counteracted by Nef. *Nature* **526,** 218–223 CrossRef Medline
23. Sood, C., Marin, M., Chande, A., Pizzato, M., and Melikyan, G. B. (2017) SERINC5 protein inhibits HIV-1 fusion pore formation by promoting functional inactivation of envelope glycoproteins. *J. Biol. Chem.* **292,** 6014–6026 CrossRef Medline
24. Shi, J., Xiong, R., Zhou, T., Su, P., Zhang, X., Qiu, X., Li, H., Li, S., Yu, C., Wang, B., Ding, C., Smithgall, T. E., and Zheng, Y. H. (2018) HIV-1 Nef antagonizes SERINC5 restriction by downregulation of SERINC5 via the endosome/lysosome system. *J. Virol.* **92,** e00196-18 CrossRef Medline
25. Shu, S. T., Emert-Sedlak, L. A., and Smithgall, T. E. (2017) Cell-based fluorescence complementation reveals a role for HIV-1 Nef protein dimerization in AP-2 adaptor recruitment and CD4 co-receptor down-regulation. *J. Biol. Chem.* **292,** 2670–2678 CrossRef Medline
26. Poe, J. A., and Smithgall, T. E. (2009) HIV-1 Nef dimerization is required for Nef-mediated receptor downregulation and viral replication. *J. Mol. Biol.* **394,** 329–342 CrossRef Medline

27. Lee, C.-H., Saksela, K., Mirza, U. A., Chait, B. T., and Kuriyan, J. (1996) Crystal structure of the conserved core of HIV-1 Nef complexed with a Src family SH3 domain. *Cell* **85,** 931–942 CrossRef Medline
28. Alvarado, J. J., Tarafdar, S., Yeh, J. I., and Smithgall, T. E. (2014) Interaction with the Src homology (SH3–SH2) region of the Src-family kinase Hck structures the HIV-1 Nef dimer for kinase activation and effector recruitment. *J. Biol. Chem.* **289,** 28539–28553 CrossRef Medline
29. Ramirez, P. W., Sharma, S., Singh, R., Stoneham, C. A., Vollbrecht, T., and Guatelli, J. (2019) Plasma membrane–associated restriction factors and their counteraction by HIV-1 accessory proteins. *Cells* **8,** 1020 CrossRef [31480747]
30. Holmes, M., Zhang, F., and Bieniasz, P. D. (2015) Single-cell and single-cycle analysis of HIV-1 replication. *PLoS Pathog.* **11,** e1004961 CrossRef Medline
31. Kerppola, T. K. (2008) Bimolecular fluorescence complementation (BiFC) analysis as a probe of protein interactions in living cells. *Annu. Rev. Biophys.* **37,** 465–487 CrossRef Medline
32. Gervaix, A., West, D., Leoni, L. M., Richman, D. D., Wong-Staal, F., and Corbeil, J. (1997) A new reporter cell line to monitor HIV infection and drug susceptibility *in vitro*. *Proc. Natl. Acad. Sci. U.S.A* **94,** 4653–4658 CrossRef Medline
33. Sharma, S., Lewinski, M. K., and Guatelli, J. (2018) An *N*-glycosylated form of SERINC5 is specifically incorporated into HIV-1 virions. *J. Virol.* **92,** e00753-18 CrossRef Medline
34. Anmole, G., Kuang, X. T., Toyoda, M., Martin, E., Shahid, A., Le, A. Q., Markle, T., Baraki, B., Jones, R. B., Ostrowski, M. A., Ueno, T., Brumme, Z. L., and Brockman, M. A. (2015) A robust and scalable TCR-based reporter cell assay to measure HIV-1 Nef-mediated T cell immune evasion. *J. Immunol. Methods* **426,** 104–113 CrossRef Medline
35. Dai, W., Usami, Y., Wu, Y., and Göttlinger, H. (2018) A long cytoplasmic loop governs the sensitivity of the anti-viral host protein SERINC5 to HIV-1 Nef. *Cell Rep.* **22,** 869–875 CrossRef Medline
36. Pye, V. E., Rosa, A., Bertelli, C., Struwe, W. B., Maslen, S. L., Corey, R., Liko, I., Hassall, M., Mattiuzzo, G., Ballandras-Colas, A., Nans, A., Takeuchi, Y., Stansfeld, P. J., Skehel, J. M., Robinson, C. V., *et al.* (2020) A bipartite structural organization defines the SERINC family of HIV-1 restriction factors. *Nat. Struct. Mol. Biol.* **27,** 78–83 CrossRef Medline
37. Pizzato, M., Helander, A., Popova, E., Calistri, A., Zamborlini, A., Palù, G., and Göttlinger, H. G. (2007) Dynamin 2 is required for the enhancement of HIV-1 infectivity by Nef. *Proc. Natl. Acad. Sci. U.S.A.* **104,** 6812–6817 CrossRef Medline
38. Cohen, G. B., Rangan, V. S., Chen, B. K., Smith, S., and Baltimore, D. (2000) The human thioesterase II protein binds to a site on HIV-1 Nef critical for CD4 down-regulation. *J. Biol. Chem.* **275,** 23097–23105 CrossRef Medline
39. Wu, Y., Olety, B., Weiss, E. R., Popova, E., Yamanaka, H., and Göttlinger, H. (2019) Potent enhancement of HIV-1 replication by Nef in the absence of SERINC3 and SERINC5. *MBio* **10,** e01071-19 CrossRef Medline
40. Sugden, S. M., Bego, M. G., Pham, T. N., and Cohen, E. A. (2016) Remodeling of the host cell plasma membrane by HIV-1 Nef and Vpu: a strategy to ensure viral fitness and persistence. *Viruses* **8,** 67 CrossRef Medline
41. Buffalo, C. Z., Sturzel, C. M., Heusinger, E., Kmiec, D., Kirchhoff, F., Hurley, J. H., and Ren, X. (2019) Structural basis for tetherin antagonism as a barrier to zoonotic lentiviral transmission. *Cell Host Microbe* **26,** 359–368. e8 CrossRef Medline
42. Schaefer, M. R., Wonderlich, E. R., Roeth, J. F., Leonard, J. A., and Collins, K. L. (2008) HIV-1 Nef targets MHC-I and CD4 for degradation via a final common β-COP–dependent pathway in T cells. *PLoS Pathog.* **4,** e1000131 CrossRef Medline
43. Stoneham, C. A., Ramirez, P. W., Singh, R., Suarez, M., Debray, A., Lim, C., Jia, X., Xiong, Y., and Guatelli, J. (2020) A conserved acidic-cluster motif in SERINC5 confers partial resistance to antagonism by HIV-1 Nef. *J. Virol.* **94,** e01554-19 CrossRef Medline
44. Shi, H., Tice, C. M., Emert-Sedlak, L., Chen, L., Li, W. F., Carlsen, M., Wrobel, J. E., Reitz, A. B., and Smithgall, T. E. (2020) Tight-binding hydroxypyrazole HIV-1 Nef inhibitors suppress viral replication in donor mononuclear cells and reverse Nef-mediated MHC-I downregulation. *ACS Infect. Dis.* **6,** 302–312 CrossRef Medline
45. Emert-Sedlak, L. A., Loughran, H. M., Shi, H., Kulp, J. L., I. I. I., Shu, S. T., Zhao, J., Day, B. W., Wrobel, J. E., Reitz, A. B., and Smithgall, T. E. (2016) Synthesis and evaluation of orally active small molecule HIV-1 Nef antagonists. *Bioorg. Med. Chem. Lett.* **26,** 1480–1484 CrossRef Medline
46. Narute, P. S., and Smithgall, T. E. (2012) Nef alleles from all major HIV-1 clades activate Src-family kinases and enhance HIV-1 replication in an inhibitor-sensitive manner. *PLoS One* **7,** e32561 CrossRef Medline